Electronic Supplementary Material (ESI) for RSC Advances.

A dipodal molecular probe for naked eye detection of trivalent cations (Al^{3+}, $Fe^{3+}$and Cr^{3+}) in aqueous medium and its applications in real sample analysis and molecular logic gate

Rukmani Chandra, Amit Kumar Manna, Kalyani Rout, Jahangir Mondal, and Goutam K. Patra*

Department of Chemistry, Guru GhasidasVishwavidyalaya, Bilaspur (C.G)

Table of Contents

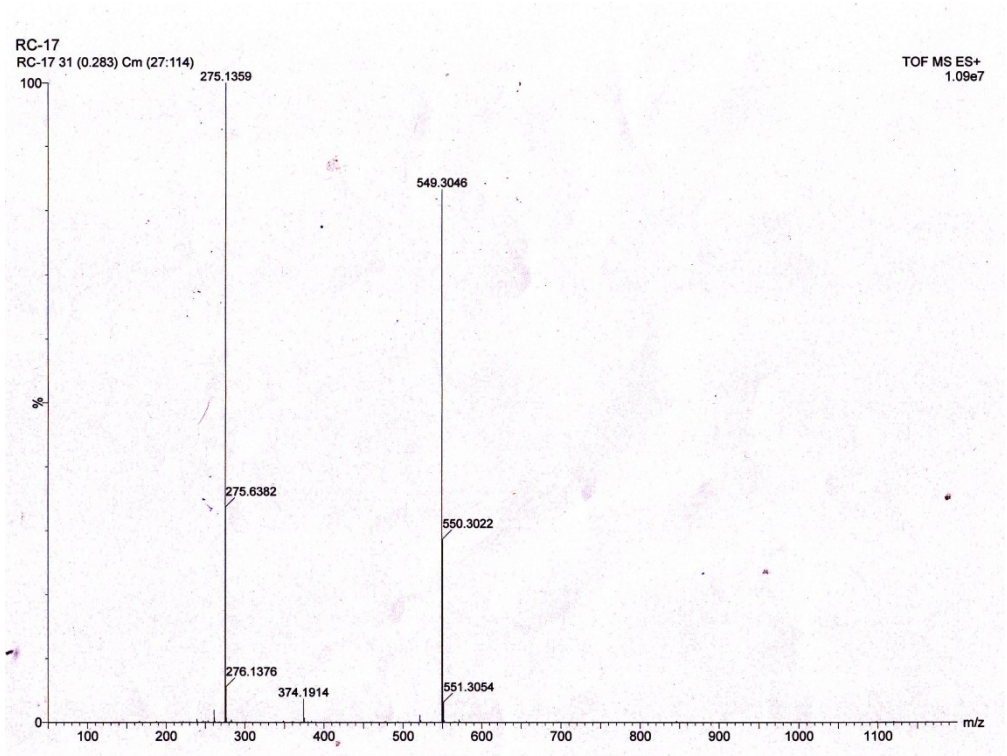

Fig. S1.ESI-MS spectra of **L.**

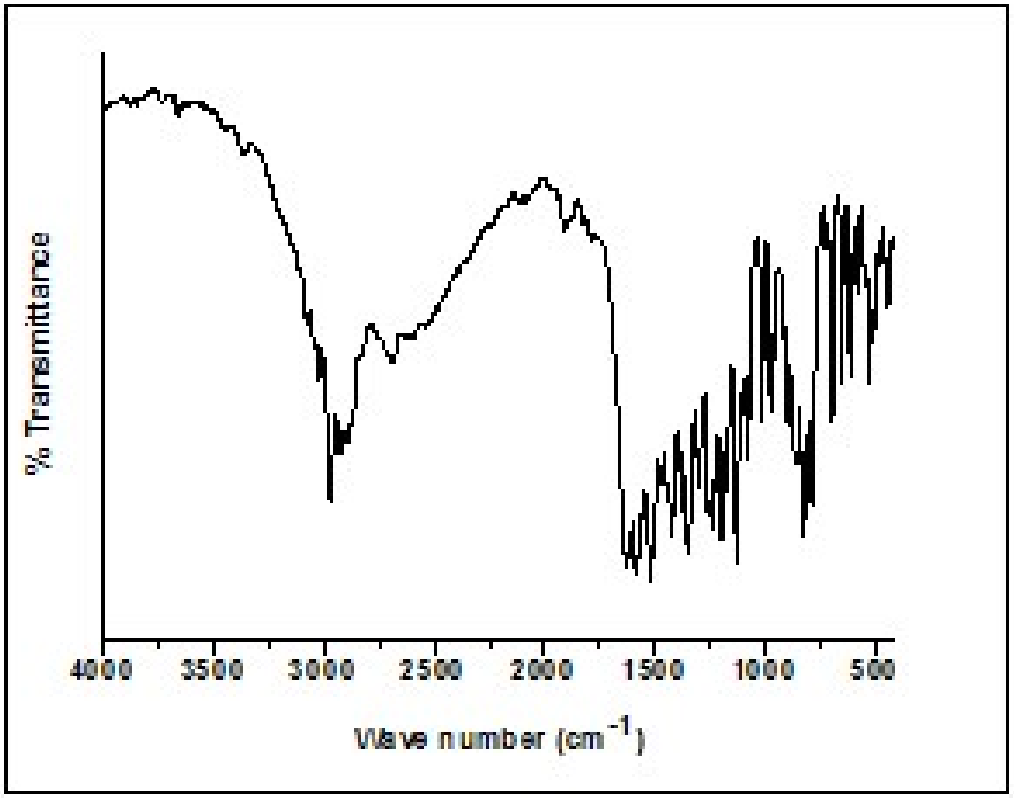

Fig. S2. FTIR spectra of **L**.

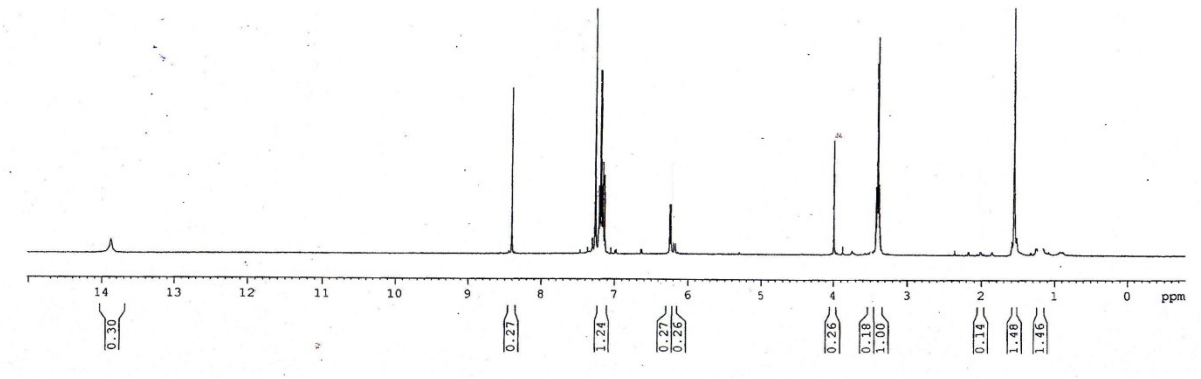

Fig. S3. ^{1}H NMR spectra of **L**

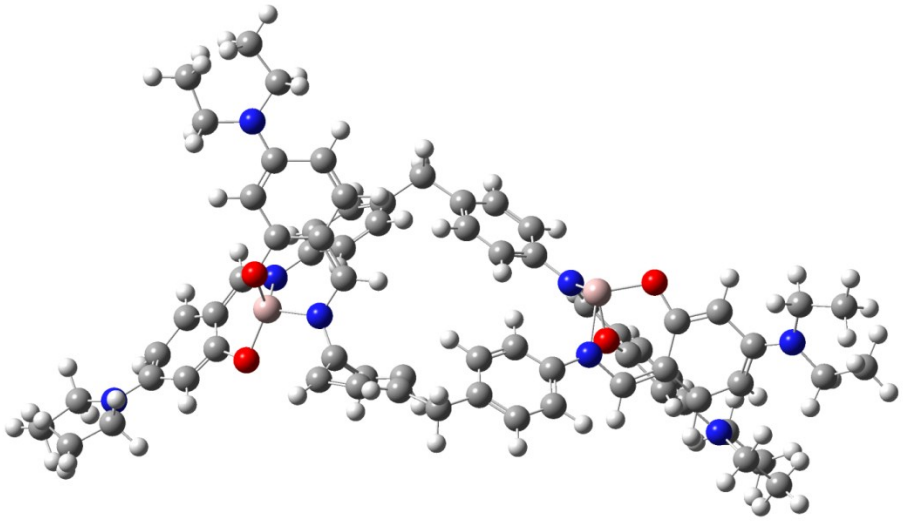

(a)

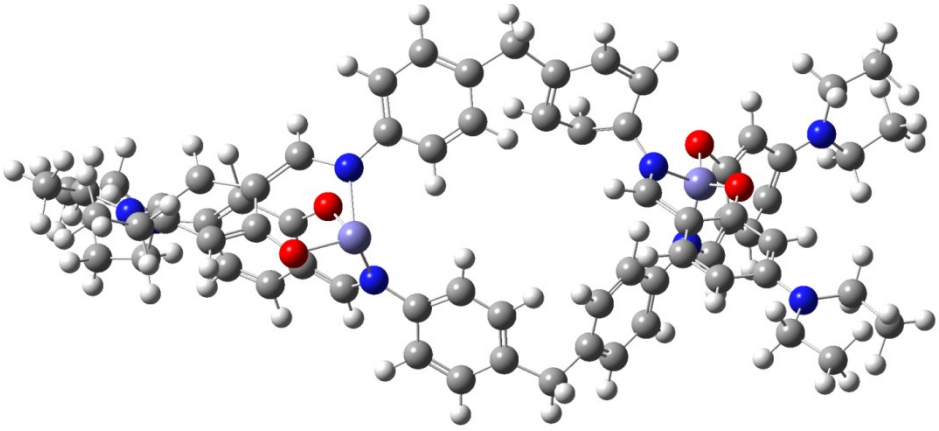

(b)

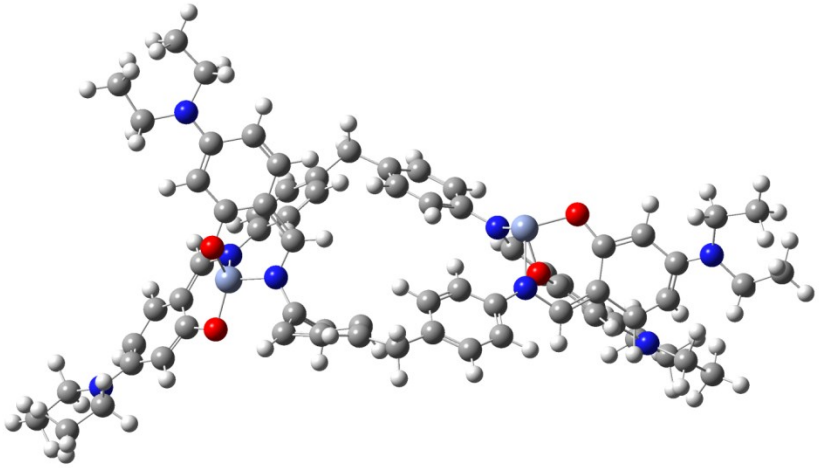

(c)

Fig. S4. Geometry optimized diagram of the molecule (a) **L** + Fe^{3+}, (b) **L**+ Al^{3+} and (c) **L** + Cr^{3+}

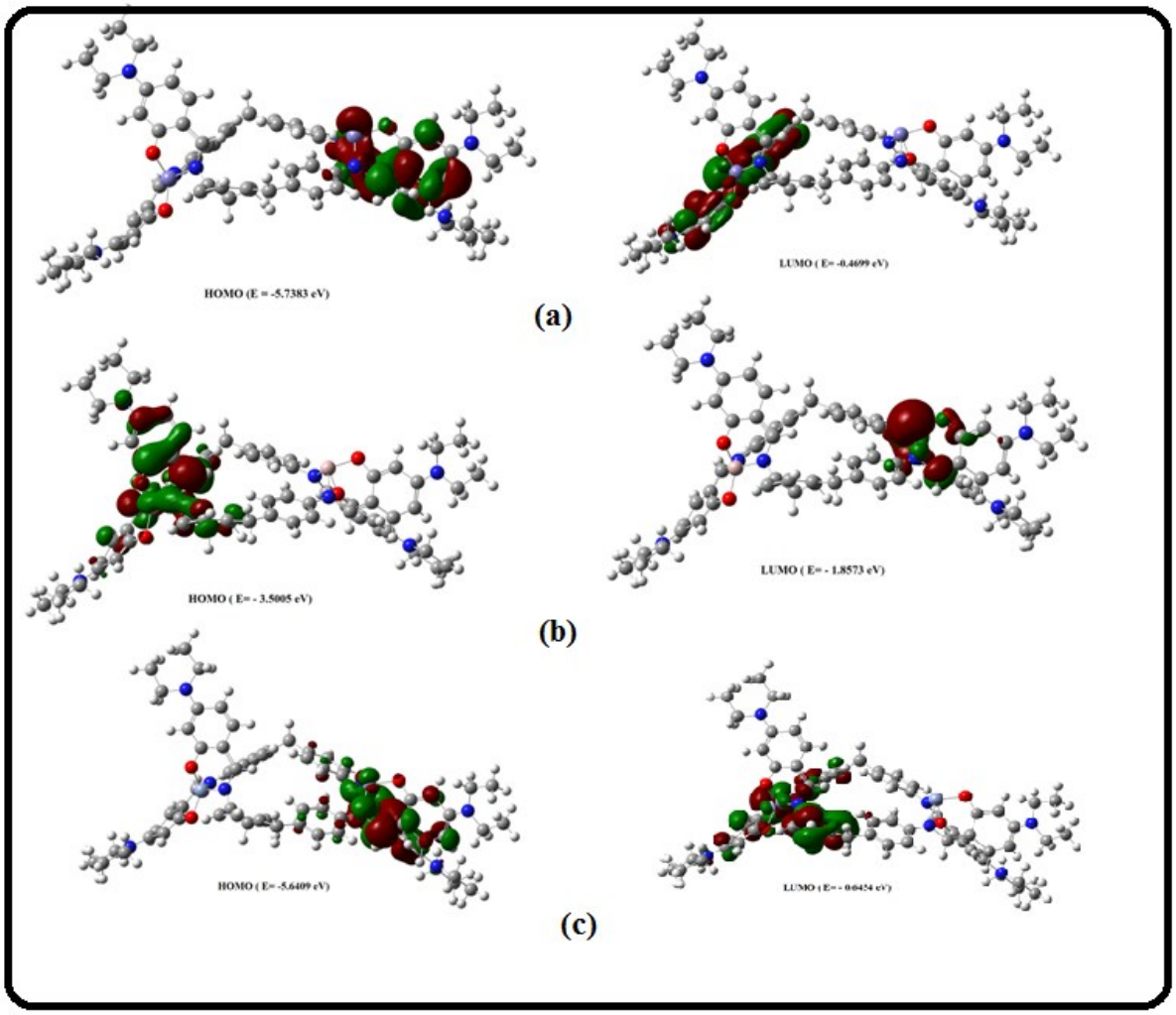

Fig. S5. The contour diagrams of selected HOMO and LUMO orbitals of (a) **L** + Fe^{3+}, (b) **L**+ Al^{3+} and (c) **L** + Cr^{3+}.

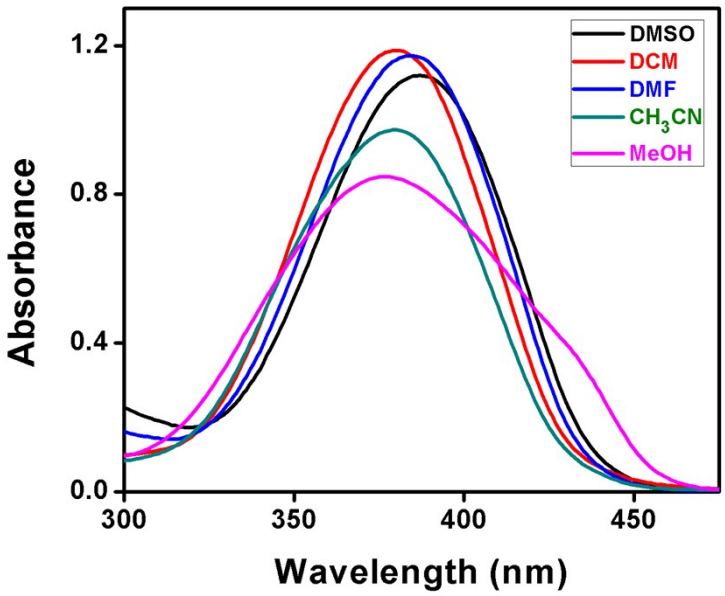

Fig. S6. Absorption spectra of **L** in different solvents.

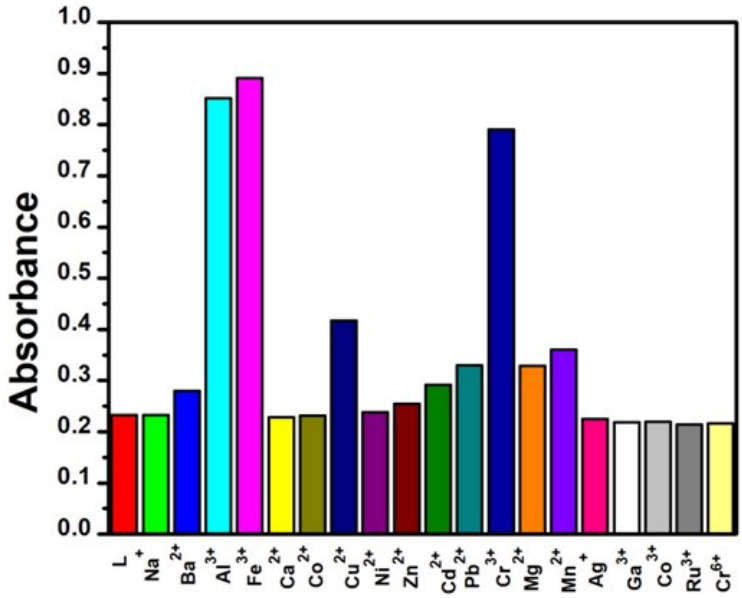

Fig. S7. The change in the absorbance intensity of **L** after addition of 1 equiv. of each of the metal ions in CH_3CN:H_2O (1:1, v/v) at 418 nm.

.

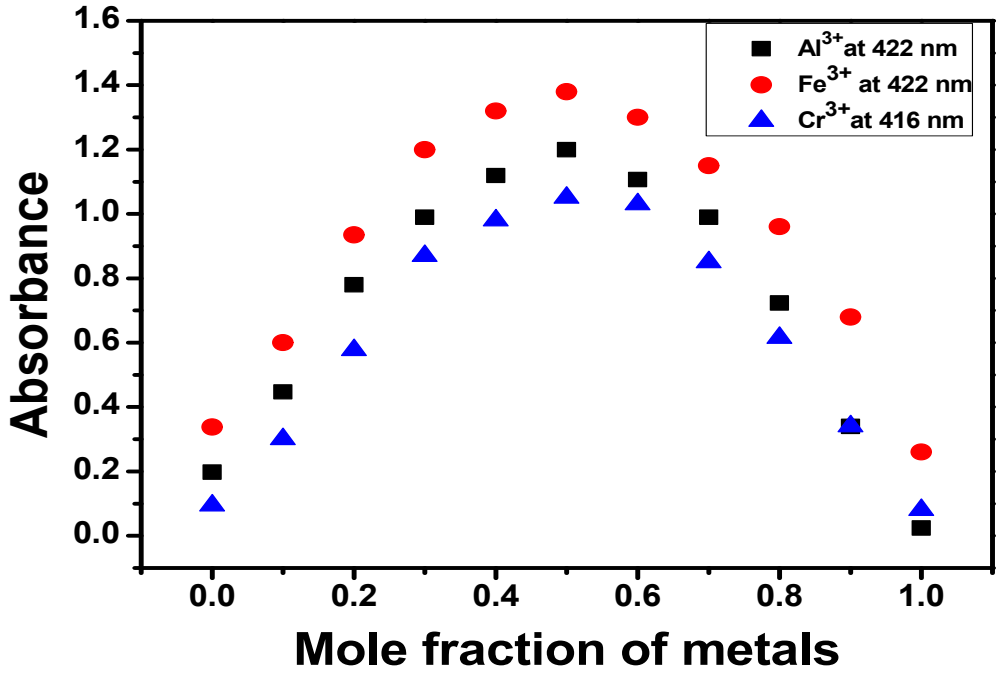

Fig. S8. Job plot for the binding of **L**with Al^{3+}, Fe^{3+} and Cr^{3+}.

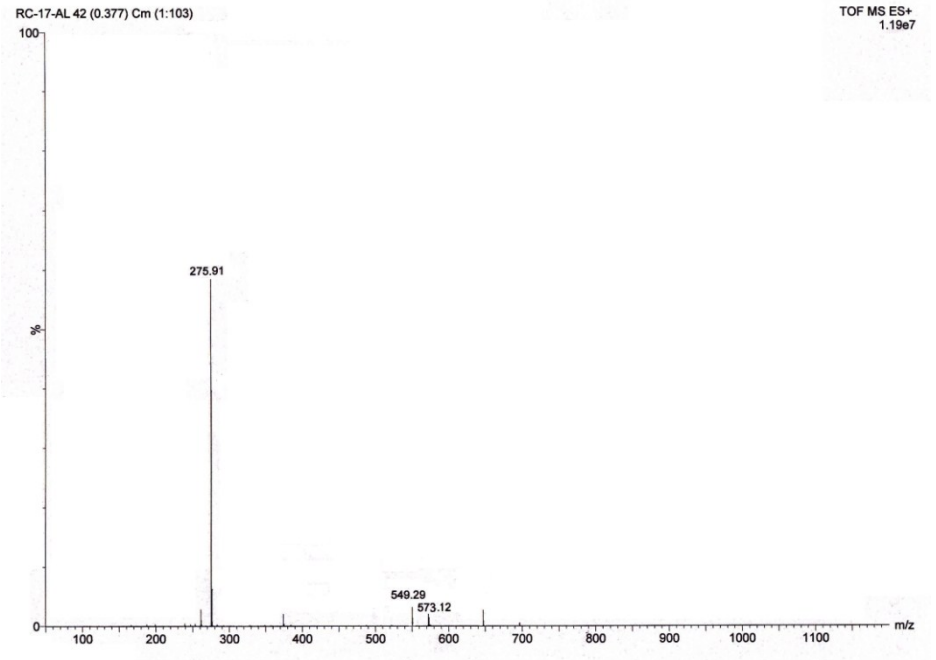

(a)

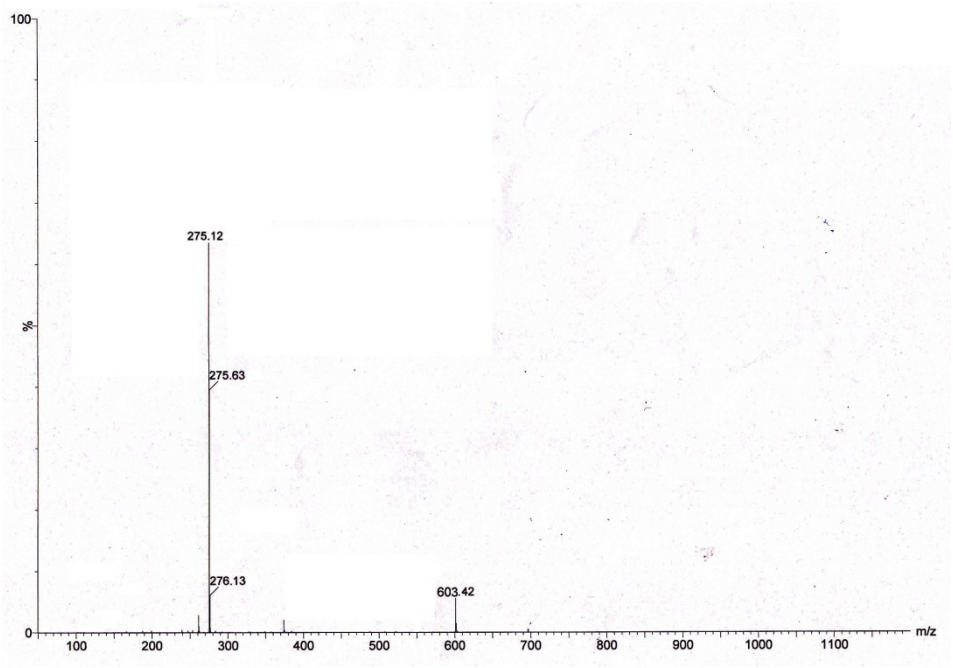

(b)

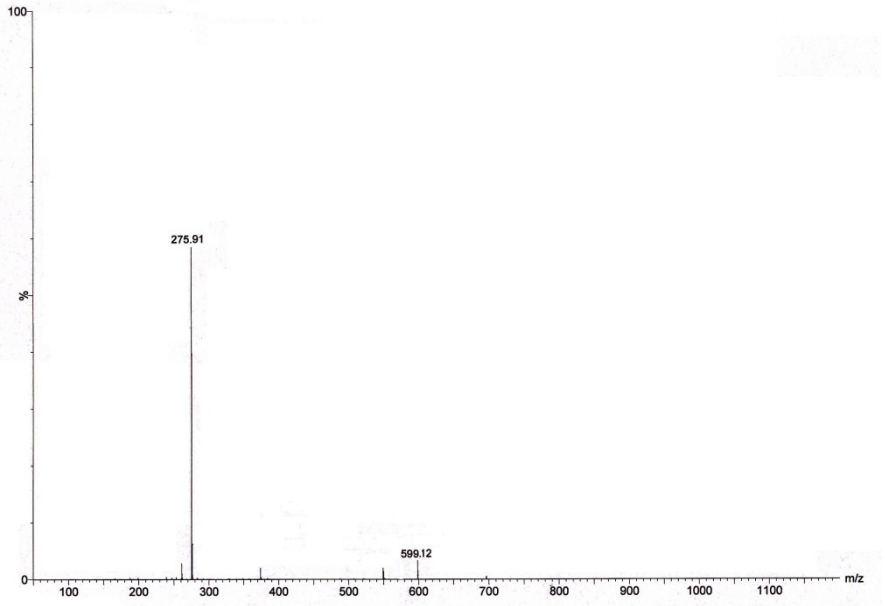

(c)

Fig. S9. ESI-MS spectra of (a) **L**-Al^{3+},(b) **L**-Fe^{3+} and (c) **L**+ Cr^{3+}

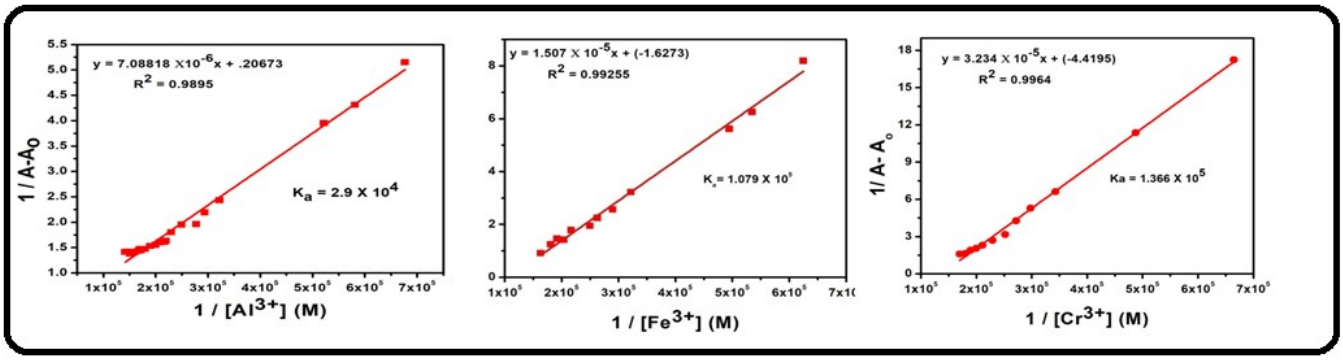

Fig. S10. Binding constants of (a) **L**-Al^{3+}, (b) **L**-Fe^{3+} and (c) **L**-Cr^{3+} complexes.

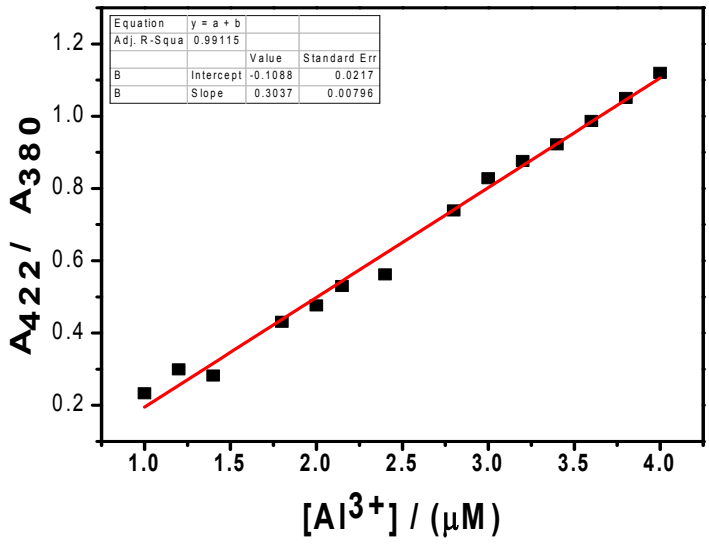

(a)

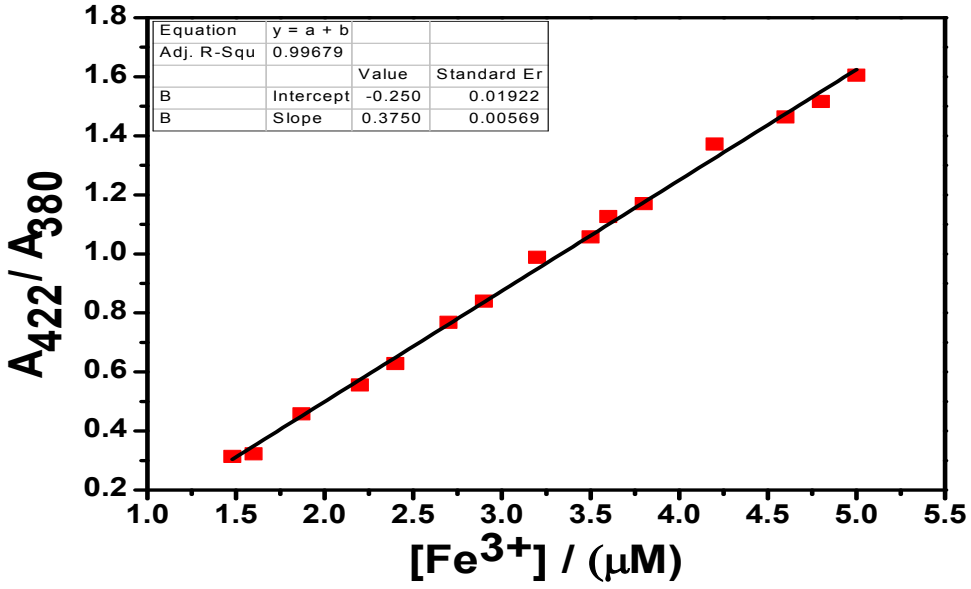

(b)

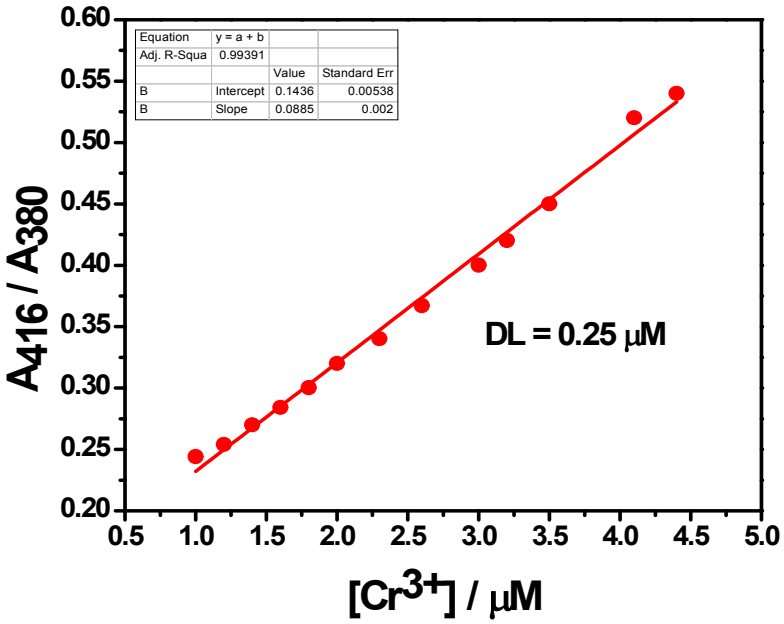

(c)

Fig. S11. Detection limits for (a)Al^{3+}, (b) Fe^{3+} and (c) Cr^{3+}

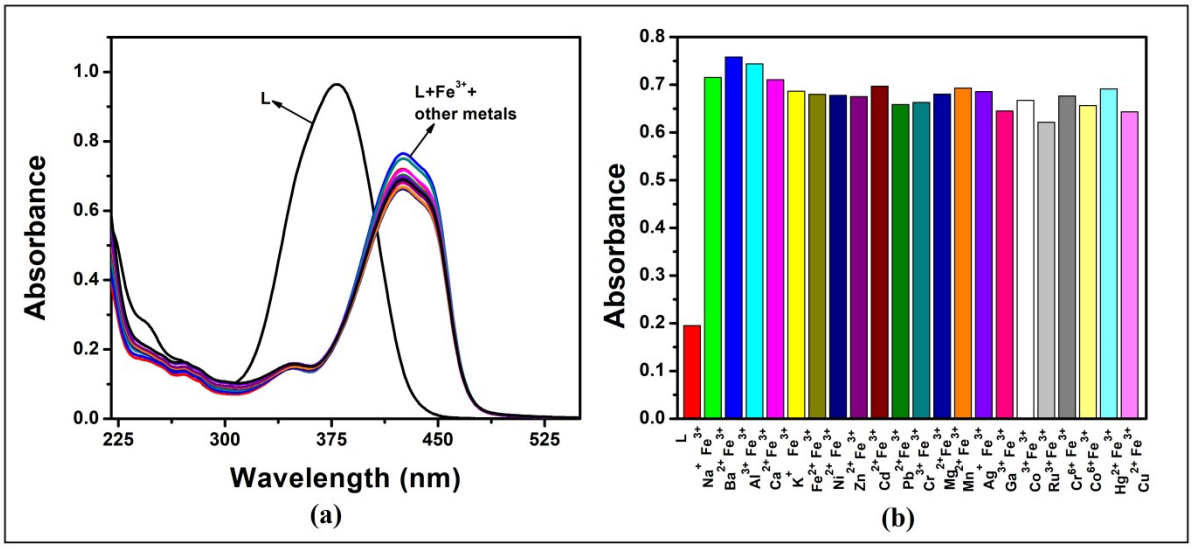

Fig. S12. Competitive selectivity of **L** towards Fe^{3+} in the presence of other metal ions (5 equiv.) (a) absorbance spectra, (b) bar diagram taking absorption intensity at 422 nm in CH_3CN/H_2O (1/1,v/v) solution.

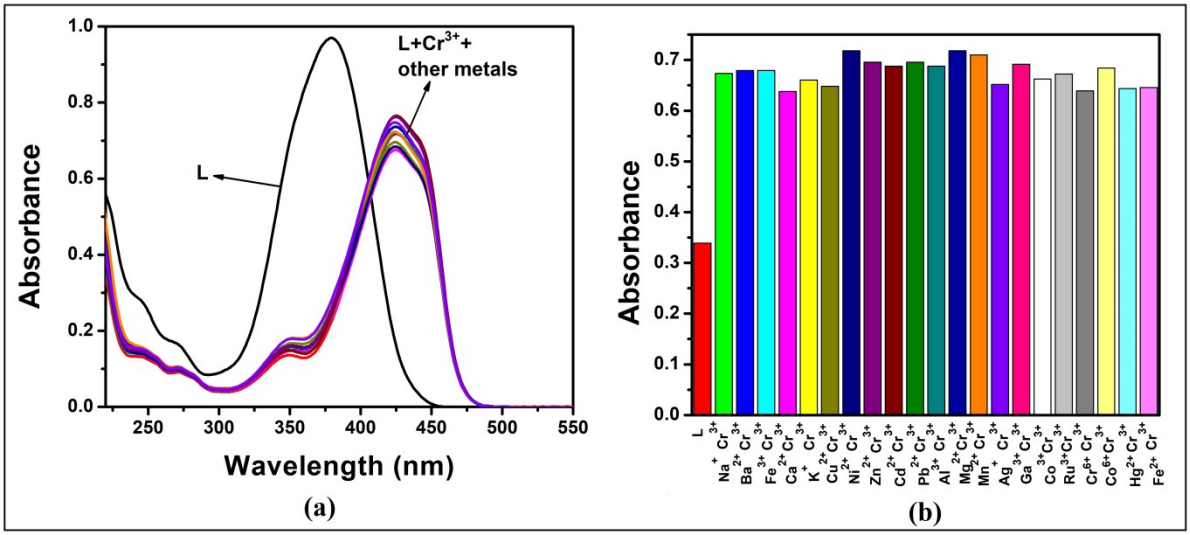

Fig. S13. Competitive selectivity of **L** towards Cr^{3+} in the presence of other metal ions (5 equiv.) (a) absorbance spectra, (b) bar diagram taking absorption intensity at 416 nm in CH_3CN/H_2O (1/1,v/v) solution.

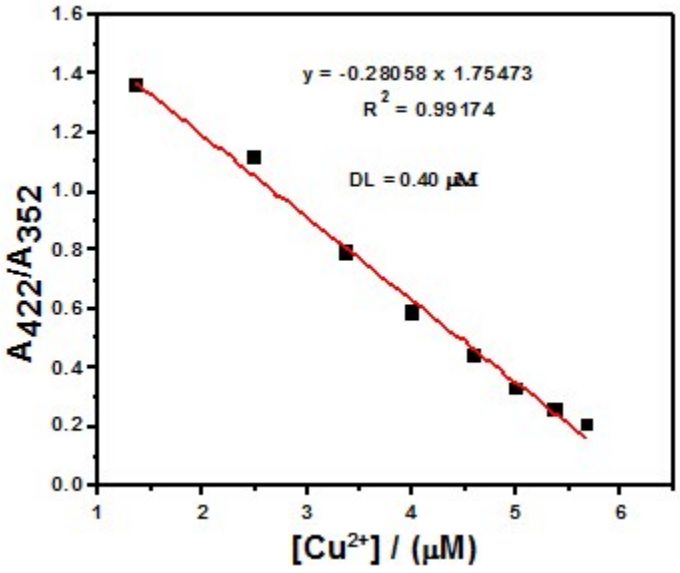

Fig. S14. Detection limit for Cu^{2+}

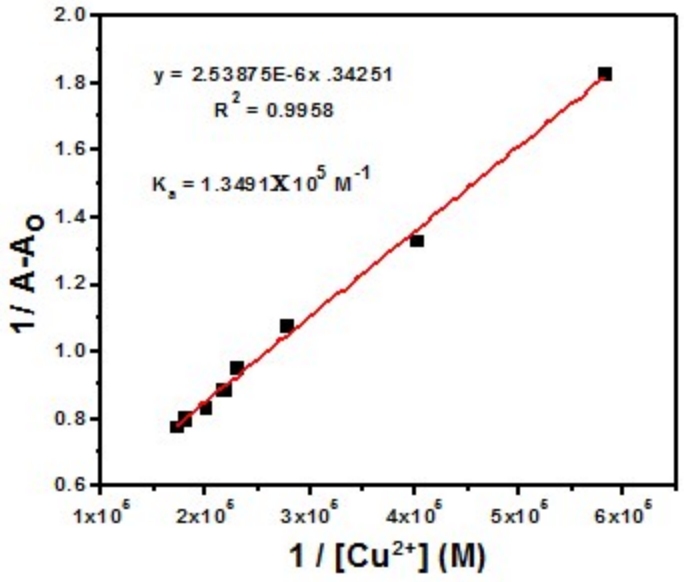

Fig. S15. Stability constant of **L′**-Cu^{2+}

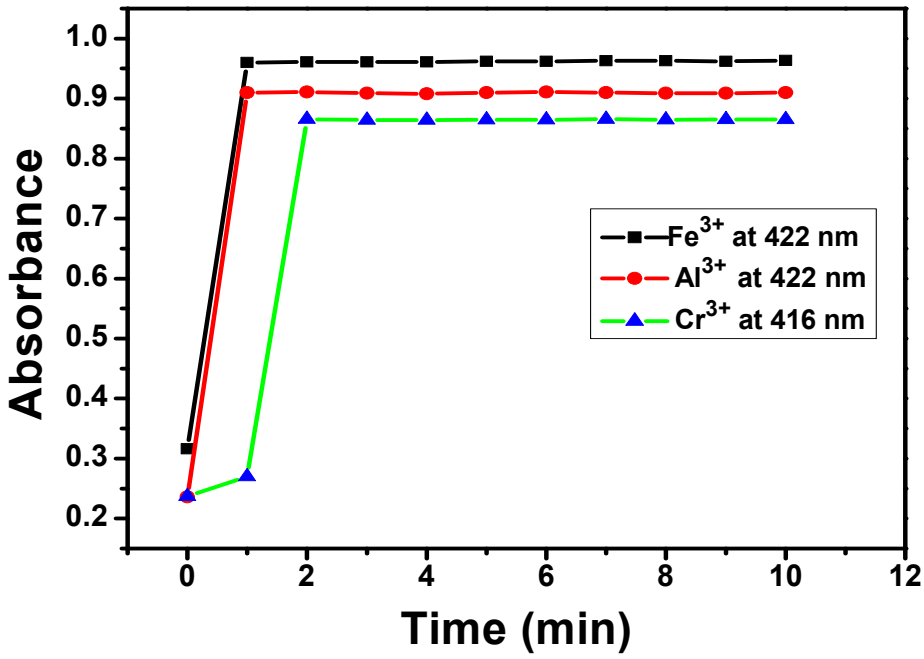

Fig. S16. Time evolution for Fe^{3+}, Al^{3+} and Cr^{3+}

Table S1. Selected optimized bond distances (Å) and angles (°) of **L**

Bond Length (Å)			Bond Angle (°)		
C1-C2	1.3916	C2-C1-C3	119.723	C57-C56-C58	116.4854

C1-C3	1.4104	C1-C2-C4	120.5773	C56-C57-C59	123.595
C2-C4	1.4061	C1-C3-C6	119.9209	C56-C57-O65	115.6621
C3-C6	1.4066	C1-C3-N50	117.4539	C59-C57-O65	120.7426
C3-N50	1.428	C6-C3-N50	122.4539	C56-C58-C60	121.8981
C4-C7	1.401	C2-C4-C7	119.5013	C57-C59-C62	118.6709
C4-C10	1.506	C2-C4-C10	120.0315	C58-C60-C62	120.6474
C6-C7	1.3966	C7-C4-C10	120.459	C59-C62-C60	118.7029
C10-C11	1.5059	C3-C6-C7	119.7877	C59-C62-N67	120.6457
C11-C12	1.4038	C4-C7-C6	120.4886	C60-C62-N67	120.6514
C11-C13	1.4034	C4-C10-C11	112.793	C62-N67-C68	122.0461
C12-C14	1.394	C10-C11-C12	120.3152	C62-N67-C69	121.941
C13-C16	1.3943	C10-C11-C13	120.2059	C68-N67-C69	116.0108
C14-C18	1.4085	C12-C11-C13	119.473	N67-C68-C70	111.5412
C16-C18	1.4084	C11-C12-C14	120.5498	C67-C69-C71	111.5894
C18-N53	1.4284	C11-C13-C16	120.5386		
C21-C22	1.4114	C12-C14-C18	119.7629		
C21-C23	1.4096	C13-C16-C18	119.769		
C21-C52	1.465	C14-C18-C16	119.9029		
C22-C24	1.3959	C14-C18-N53	117.2902		
C22-O30	1.375	C16-C18-N53	122.6447		
C23-C25	1.3863	C22-C21-C23	116.5109		
C24-C27	1.4162	C22-C21-C52	120.6621		
C25-C27	1.4233	C23-C21-C52	122.827		
C27-N32	1.4047	C21-C22-C24	123.4485		
N32-C33	1.49	C21-C22-O30	115.7105		
N32-C34	1.4908	C24-C22-O30	120.8403		

C33-C35	1.5281	C21-C23-C25	121.8034
C34-C36	1.5277	C22-C24-C27	118.8337
N50-C51	1.3004	C23-C25-C27	120.7744
C51-C56	1.4634	C24-C27-C25	118.6246
C52-N53	1.3	C24-C27-N32	120.5963
C56-C57	1.4115	C25-C27-N32	120.6017
C56-C58	1.4109	C27-N32-C33	119.8171
C57-C59	1.3948	C27-N32-C34	119.6529
C57-O65	1.3751	C33-N32-C34	114.8051
C58-C60	1.3845	N32-C33-C35	113.9605
C59-C62	1.4189	N32-C34-C36	113.9522
C60-C62	1.4266	C3-N50-C51	121.5536
C62-N67	1.3891	N50-C51-C56	120.231
N67-C68	1.4859	C21-C52-N53	120.1215
N67-C69	1.4866	C18-N53-C52	121.5511
C68-C70	1.5286	C51-C56-C57	120.728
C69-C71	1.5282	C51-C56-C58	122.7865